



RESEARCH ARTICLE

Chandipura virus changes cellular miRNome in human microglial cells

Meghna Agrawal¹ | Meghana Rastogi¹ | Smriti Dogra¹ | Neha Pandey¹ | Anirban Basu² | Sunit K. Singh PhD¹

¹Molecular Biology Unit, Institute of Medical Sciences, Banaras Hindu University, Varanasi, India

²Division of Cellular and Molecular Neuroscience, National Brain Research Centre, Manesar, India

Correspondence

Sunit K Singh, PhD, Molecular Biology Unit, Institute of Medical Sciences, Banaras Hindu University, Varanasi, Uttar Pradesh 221005, India.

Email: sunitsingh2000@bhu.ac.in; sunitsingh2000@gmail.com

Funding information

Department of Biotechnology, Ministry of Science and Technology, Grant/Award Numbers: BT/PR27501/MED/122/142/2018, BT/HRD/35/01/02/2014

Abstract

Chandipura virus (CHPV) is a neurotropic virus, known to cause encephalitis in humans. The microRNAs (miRNA/miR) play an important role in the pathogenesis of viral infection. The present study is focused on the role of miRNAs during CHPV (strain 1653514) infection in human microglial cells. The deep sequencing of CHPV-infected human microglial cells identified a total of 12 differentially expressed miRNA (DEMs). To elucidate the role of DEMs, the target gene prediction, Gene Ontology term (GO Term), pathway enrichment analysis, and miRNA-messenger RNA (mRNA) interaction network analysis was performed. The GO terms and pathway enrichment analysis provided 146 enriched genes; which were involved in interferon response, cytokine and chemokine signaling. Further, the WGCNA (weighted gene coexpression network analysis) of the enriched genes were discretely categorized into three modules (blue, brown, and turquoise). The hub genes in the blue module may correlate to CHPV induced neuroinflammation. Altogether, the miRNA-mRNA interaction network and WGCNA study revealed the following pairs, hsa-miR-542-3p and FAF1, hsa-miR-92a-1-5p and MYD88, and hsa-miR-3187-3p and TNFRSF21, which may contribute to neuroinflammation during CHPV infection in human microglial cells.

KEYWORDS

Chandipura virus, deep RNA sequencing, human microglial cells, microRNAs, module analysis, neuroinflammation, Rhabdoviridae, weighted gene coexpression analysis

1 | INTRODUCTION

Chandipura virus (CHPV) (family *Rhabdoviridae*, genus *Vesiculovirus*) is an Arbovirus, transmitted through infected sand flies (*Phlebotomus* spp. and *Sergentomyia* spp.).¹ The CHPV was first isolated in the Chandipura district, Maharashtra in 1965 from the serum of patient with febrile illness.² CHPV is a neurotropic virus and infects central nervous system (CNS).¹ Children below the age of 15 years are more susceptible to CHPV infection, with case-fatality rate of 55% to 77%.² CHPV-infected patients show symptoms similar to encephalitis

which includes altered sensorium, acute fever, seizures, decerebrate posture, grade IV coma, and ultimately death.¹

CHPV is a negative single-stranded RNA (-ssRNA) virus with a genome size of ~11 kb. The CHPV genome comprises five genes, which encode for glycoprotein (G), matrix protein (M), nucleoprotein (N), phosphoprotein (P), and large polymerase protein (L). The nonsegmented single-stranded RNA genome of CHPV is encapsulated by the viral nucleocapsid (N) protein; which forms a helical ribonucleoprotein complex to facilitate virus replication and propagation.³

CHPV may enter CNS either through nerve endings of motor neurons or through "Trojan Horse" mechanism mediated by infected monocytes.⁴ The neurons, monocytes, and B lymphocytes are the primary targets of the CHPV infection. The microglial cells are the resident macrophages of CNS, which are involved in immune surveillance, phagocytosis, and antigen presentation.⁵ CHPV infection in CNS leads to microglial activation and induces neuroinflammation.⁶ The elevated levels of cytokines and chemokines have been reported in brain supernatant of mice⁷ during acute or persistent CHPV infection. The neuroinflammatory responses in CNS may promote disruption of the blood-brain barrier (BBB) and infiltration of T and B lymphocytes, dendritic cells, and natural killer cells from the periphery to the CNS, which may lead to inflammation.⁵

The microRNAs (miRNAs) are the group of noncoding RNAs, 19 to 22 nucleotides in length, which are involved in post-transcriptional gene regulation.⁸ The miRNAs bind to 3'-untranslated regions (3'-UTR) of their target genes, thereby, regulating their expression either by inhibiting its stability or translation. The roles of miRNAs have been reported in various biological processes like signal transduction, cell proliferation, stress response, apoptosis, and so forth. The miRNAs have been reported as the key players in disease progression during viral infection, neuroinflammation, and neurodegeneration.^{5,9-11} and so forth. There are no published reports on miRNA expression pattern in human microglial cells during CHPV infection.

In the present study, the microglial cells were infected with CHPV (strain 1653514) and the virus replication was determined through plaque assay (Figure 1A). Further, the miRNA expression profile of CHPV-infected human microglial cells (24 hours postinfection) was

generated using deep sequencing to identify the differentially expressed microRNAs (DEMs). The predicted and the validated target genes listed in tables for each DEMs have been obtained through target gene prediction databases. In addition, the GO term and pathway enrichment analysis have also been performed. The miRNA-mRNA interaction networks have been constructed for the screened target genes with their corresponding DEMs through the enrichment analysis. The weighted gene coexpression network (WGCNA) of the genes obtained through the enrichment analysis was constructed to understand the interaction between the genes. The significant modules and key genes correlated to neuroinflammation were identified through weighted gene coexpression network analysis (WGCNA) during CHPV infection in human microglial cells (Figure 1B). Therefore, the present study provides a bigger picture of miRNAs perturbation in human microglial cells during CHPV infection.

2 | MATERIALS AND METHODS

2.1 | Cell culture, virus infection, virus titration, and RNA extraction

The human microglial cells were infected with CHPV (strain 1653514) at multiplicity of infection (MOI) 0.1 in incomplete Dulbecco's modified Eagle's medium (DMEM) (Gibco, Rockville, MA) supplemented with 100 U/mL of penicillin, 100 mg/mL streptomycin and 29.2 mg/mL L-glutamine (Pen-strep, Gibco, Rockville, MA) for 1 hour, at National Brain Research Centre (NBRC), Manesar, India. The incomplete cell culture media was replaced by complete DMEM supplemented with 10% fetal bovine serum (FBS) post infection and

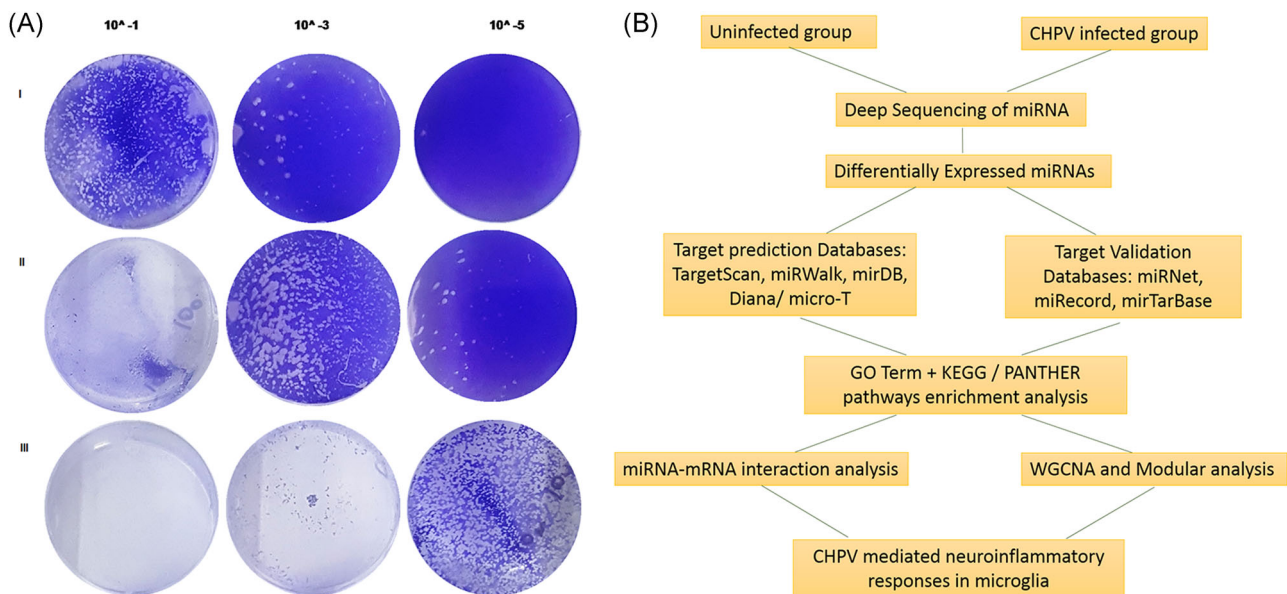


FIGURE 1 The workflow of study design and data analysis of CHPV-infected microglia. A, The supernatant of CHPV-infected human microglia were collected at (i) 10, (ii) 18, and (iii) 24 hours post infection and was titrated on Vero cells by plaque assay. The plaque assay demonstrates CHPV infects and replicates in human microglial cells in a time-dependent manner determined at different dilutions (10^{-1} , 10^{-3} , and 10^{-5}). B, The flowchart representing the outline for miRNA-mRNA interaction network and weighted gene coexpression network analysis of CHPV-infected microglia. CHPV, Chandipura virus; GO, Gene Ontology; KEGG, Kyoto Encyclopedia of Genes and Genomes; miRNA, microRNA; mRNA, messenger RNA; WGCNA, weighted gene coexpression network analysis

the culture was kept for incubation for 24 hours post infection. The culture supernatant was aspirated for plaque assay and the cell pellets were used for RNA isolation.

The stock supernatant of CHPV-infected microglial cells was serially diluted to 10^{10} dilutions in serum-free DMEM and each dilution was added to a monolayer of Vero cells plated on six-well plates. After 2 hours of incubation with the respective dilutions, the supernatants were removed and washed twice with $1\times$ phosphate-buffered saline (PBS) to avoid multiple infection cycles. 2 mL of agarose overlay (2% agarose; Roche, Mannheim, Germany), 2 mL $2\times$ DMEM (Sigma-Aldrich) supplemented with 10% FBS was added to each well. The 10% PFA (paraformaldehyde) was added post-incubation period for fixation of the cells for further analysis. Subsequently, the overlay was removed, and cells were stained with crystal violet and the plaques were counted (Figure 1A).

The total RNA was isolated from mock-infected and CHPV-infected microglial cells by using the miRNeasy kit (Qiagen, Hilden, Germany). The RNA concentration and its integrity were evaluated by NanoDrop, MA (A260/A280 and A260/A230 ratios) for deep sequencing of miRNA.

2.2 | The miRNA expression profile of CHPV-infected microglial cells

The microRNA expression profiling was performed through deep sequencing on IlluminaNextSeq platform. The 500 ng of total RNA of uninfected and CHPV-infected microglial cells were used as input to make the small RNA library (<30 nt) using NEBNext kit (NEB, MA). The purified fractions of the small RNA libraries (<30 nt) were obtained using AMPure XP beads (Beckman, CA). The final fractionalized libraries were quantified individually and multiplexed for template preparation for sequencing on IlluminaNextSeq platform. The sequence was analyzed by using the comprehensive analysis pipeline for miRNA sequencing data. The clean data was obtained by removing the low-quality bases; which were dynamically trimmed at 3' end for adapter sequence and removing sequences <17 nt. The reads were aligned with Bowtie software and miRDeep2. The Bowtie software was used to compare the reads with the miRBase to identify annotated miRNAs. The miRDeep2 quantified and predicted novel miRNAs, which were not assigned by miRBase annotation. The miRNA profile was further used to identify differentially expressed miRNA between the uninfected and CHPV-infected microglia cells. The edgeR tool was used for empirical analysis of digital gene expression data using Bayes estimation. The P value distribution was used to analyze the magnitude of difference between the mock-infected and CHPV-infected conditions.

2.3 | Target analysis of differentially expressed microRNAs

The putative gene targets for differentially expressed miRNAs were predicted by using TargetScan version 7.2 (www.targetscan.org/vert_72/), miRWalk 2.0 (zmf.umh.uni-heidelberg.de/apps/zmf/mirwalk2/miR-retsyst-self.html), miRDB (www.mirdb.org/), and DianaTools (http://diana.imis.athena-innovation.gr/DianaTools/index.php?r=microT_CDS/

index) databases. These freely available online databases follow different algorithm and scoring pattern for gene prediction. The TargetScan version 7.2 uses P_{CT} score (higher the score, significant the target) and the conservation of seed sequence either at 5'- or 3'-UTR region. The minimum P_{CT} score limit cut off for inclusion of the target in the analysis was |0.01| (module of 0.01). The miRWalk database provides significant P value, lower the value significant the target, while in miRDB, the score ranges from 50 to 100, higher the score; significant the target. DIANA tools micro-T-CDS provides the confidence score; higher the score, significant the target. The Venn diagram was generated using "Draw Venn Diagram" tool provided by Bioinformatics and Evolutionary Genomics (<http://bioinformatics.psb.ugent.be/webtools/Venn/>) by uploading the putative target genes of DEMs from each database.

In addition, validated target genes miRNA were recorded using miRecords (<http://c1.accurascience.com/miRecords/>), miTarBase (<http://mirTarbase.mbc.nctu.edu.tw/>), and miRNet (<http://www.mirnet.ca/>). To eliminate false discovery rate by the validated target databases, the target genes reported in these databases were manually curated and the target genes which were experimentally validated by quantitative polymerase chain reaction (q-PCR), Western blot analysis, or luciferase reporter assays were only included.

2.4 | GO term and pathway enrichment analysis

The Database for Annotation, Visualization, and Integrated Discovery (DAVID v6.8) (david.ncifcrf.gov/) was used for enrichment analysis. The functionally enriched GO (Gene Ontology) terms facilitate the interpretation of the functional aspects of genes and their association to a biological process, molecular functions or cellular components. The KEGG (Kyoto Encyclopedia of Genes and Genomes) and PANTHER pathways enrichment analysis highlighted the over-represented target genes involved in different pathways in reference to the human background. The combined list of predicted and validated gene targets were submitted to DAVID v6.8 and PANTHER databases for the analysis. The enriched GO terms and pathways were selected on the basis of fold enrichment and P values. The P value in the enrichment analyses was considered only when their statistical significance values were less than 0.05 (Benjamini and Hochberg corrected P -value) and the fold enrichment was more than five.

The validation of predicted enriched genes was performed through Western blot analysis. The harvested cell pellets of CHPV uninfected and infected were lysed in radioimmunoprecipitation assay buffer (150 mM NaCl, 50 mM Tris-HCl, pH 7.5, 1% NP-40, 0.5% sodium deoxycholate, 0.1% sodium dodecyl sulfate) with $1\ \mu\text{M}$ phenylmethylsulfonyl fluoride and $1\times$ protease inhibitor cocktail (G-Biosciences, St Louis, MO). The cell lysate was sonicated, and protein was quantified by using bicinchoninic acid assay (Novagen, Merck, MA). The equal amounts of protein were loaded into each well, resolved on 12% SDS-polyacrylamide gel electrophoresis gel, and transferred on polyvinylidene difluoride membrane, the blocking of membrane was performed with 5% skimmed milk, incubated with antibodies (AKT [1:1000; #2920S; CST, MA], PTEN [1:1000; #9559S; CST, MA], TRAF3 [1:1000; #NB100-5665-4SS; Novus, CO],

TRIM21 [1:1000; #sc_253251; Santa Cruz, CA], β -tubulin [1:1000; #ab6046; Abcam, Cambridge, MA]), and secondary antibody conjugated to horseradish peroxidase-against mouse and rabbit (1:30 000) were used for visualization in ChemiDoc (Azure Biosystems, CA).

2.5 | Construction of miRNA-mRNA interaction network

The miRNA-mRNA interaction study was performed to analyze the relationship between miRNA and gene. The network was constructed on the basis of direct interaction of DEMs with their corresponding gene targets, obtained from DAVID by performing enrichment analysis. The Cytoscape version 3.6.1 was used for the construction and visualization of the miRNA-mRNA interaction network.

2.6 | Gene expression data

The pathway enrichment data revealed the genes which were involved in neuroinflammation during CHPV infection. Since there is no report available on the gene expression profile data of CHPV infection, the gene expression profile data of the closely related neurotropic ssRNA viruses were used to understand the roles of genes involved in the neuroinflammation, which were revealed during the enrichment analysis of the putative genes. The previous reports have shown interferon- γ (IFN- γ) as a potential player in inducing neuroinflammation, therefore, the IFN- γ gene expression profile was selected to understand the neuroinflammatory responses in CHPV infected microglial cells.⁷ The previously published mRNA data sets of C57BL/6J mice, *Macaca fascicularis*, *Mus musculus*, and microglial cells stimulated with Lassa virus (LASV), Rabies virus (RABV), vesicular stomatitis virus (VSV), and human recombinant IFN- γ were downloaded from gene expression omnibus (GEO data sets—GSE30577, GSE41752, GSE44331, and GSE1432). In addition, gene expression profile for human recombinant tumor necrosis factor- α (rTNF- α)- and rIFN- γ (recombinant IFN- γ)-induced astrocytes and endothelial cells were also downloaded from GEO data sets (GSE45880 and GSE3920) to study the neuroinflammatory events in CHPV-infected microglial cells. The description of samples, duration post infection/stimulation (hours) and platform accession numbers of above discussed GEO data sets have been listed in Table S6. The above mentioned GEO data sets were already validated through qPCR, Western blot analysis, immunofluorescence, and ELISA assays in the published literature.

2.7 | Weighted gene coexpression network analysis

The weighted gene coexpression networks were built using the WGCNA package in the R computing statistical tool. The network construction was performed by using the block-wise module function of WGCNA. The data sets used for network construction compared the functionally enriched gene targets of CHPV-infected microglial

cells with the gene expression profiles of GSE30577, GSE41752, GSE44331, and GSE1432. The simulated gene expression profile for CHPV-infected microglial cells is mentioned in Table S7.¹² The simulated gene expression profile for CHPV-infected microglial cells were compared to the LASV, VSV, and RABV infection and IFN- γ induced cells. The network was constructed by computing pair-wise correlation matrix for each set of genes and adjacency matrix was calculated by raising the correlation matrix to soft threshold power. The power was determined to construct the network in a scale-free topology. Further, a robust measure of network interconnectedness (topological overlap measure) was calculated based on the adjacency matrix for each pair of genes. The topological overlap based dissimilarity was used as input for average linkage hierarchical clustering analysis. The modules were defined as branches of the resulting clustering tree. The hybrid dynamic tree-cutting was used to cut the branches of the clustering tree, which leads to robustly defined modules. The dendrogram was cut at a split-cut height 15, module merging at 0.25 and minimum module size 25 to obtain the moderately large and distinct modules. Each module was summarized by the first principal component (kME), which was used to assess biological, genetic, pathological, clinical trait during disease progression. The kME values of each module were compared to the gene expression profile of GEO data sets GSE45880 and GSE3920. The module membership measure was also determined for each gene of the module, which defined the hub genes of the module on the basis of connectivity in the module and position in the network.

3 | RESULTS

3.1 | The CHPV infection in human microglial cells perturbs the miRNA expression

The genome-wide miRNA expression profile of the two biological replicates of CHPV-infected and -uninfected microglia was analyzed using deep sequencing. The three small RNA libraries from the corresponding isolated samples were sequenced and multiplexed by IlluminaNextSeq platform. In total, 20.529570, 14.998507, and 22.207227 raw reads per million (rpm) were generated from the isolated RNA from uninfected microglial cells and the two biological replicates of CHPV-infected microglial cells, respectively. After removing low-quality reads and adapters, 15.450798, 11.011722, and 16.043936-rpm clean reads were obtained from uninfected samples and CHPV-infected samples, respectively. The clean reads were matched with precursor-miRNA reads; which represented 3.421684-rpm mature sequences in uninfected samples, 2.785068 and 4.348262-rpm mature sequences in CHPV-infected samples, respectively. In total, 566 known miRNAs were detected in the CHPV-infected and -uninfected human microglial cells. The expression difference of miRNA between the uninfected and infected groups has been represented by non-symmetrical distribution in the volcano plot (Figure S1).

The miRNA expression level with more than 1.5 fold change FDR (false discovery rate) ($P < 0.05$) was considered as differentially

TABLE 1 The differentially expressed miRNAs (DEMs) in CHPV-infected microglial cells

S. No.	DEMs	Fold change	Upregulated/Downregulated	P value (FDR)
1	hsa-miR-3607-3p	2.50701	Upregulated	0.0468042
2	hsa-miR-542-3p	1.55835	Upregulated	0.0138364
3	hsa-miR-618	-1.52103	Downregulated	0.0165557
4	hsa-miR-1273f	-1.69417	Downregulated	0.0334406
5	hsa-miR-597-3p	-1.70806	Downregulated	0.0420147
6	hsa-miR-92a-1-5p	-1.71507	Downregulated	0.0193345
7	hsa-miR-935	-1.86722	Downregulated	0.0126828
8	hsa-miR-3187-3p	-1.92284	Downregulated	0.0253608
9	hsa-miR-501-5p	-2.02338	Downregulated	0.0181897
10	hsa-miR-3687	-2.07646	Downregulated	0.017682
11	hsa-miR-2682-3p	-2.17919	Downregulated	0.0377138
12	hsa-miR-324-5p	-2.93509	Downregulated	0.0353365

Abbreviations: CHPV, Chandipura virus; FDR, false discovery rate; miR, miRNA.

expressed miRNAs (DEMs). Out of 566 known miRNAs, a subset of 12 miRNAs was found to be differentially expressed in which two miRNAs were upregulated and 10 miRNAs were downregulated during CHPV infection in human microglia cells (Table 1).

3.2 | The target gene prediction of DEMs through bioinformatics databases

The target gene prediction of the 12 DEMs was performed using prediction databases (TargetScan, miRDB, miRanda, and Diana micro-T). The target genes contain a unique binding site for their corresponding miRNAs, which follows the Watson-Crick base-pairing principle. However, the prediction software often suffers from high false-positive discovery rate, the intersection of the target gene with at least two major algorithms were considered as putative target (Figure 2). The selection criteria for target genes were based on (1) the role of genes in viral infection, (2) significant scores of the target genes in the prediction databases, and (3) the presence of the genes in at least two databases. During the target screening, a total of 38 359 genes were predicted, out of which 362 were selected for further analysis (Table S1). There were 67 putative genes; which were identified by all the four target prediction databases. The top seven genes (LPAR1, ILK, MARCKSL1, IL7R, PTPN2, ELAVL1, and MAP4K3) were selected out of 67 genes based on their prediction scores.

There were several genes targeted by DEMs, which have been validated experimentally through q-PCR, Western blot analysis, and reporter assays, but are not reported in the target prediction software. The target prediction databases can eliminate the miRNA-target genes; which are not under the criteria of the stringent algorithm of the target prediction databases. Therefore, the validated genes targets for 12 DEMs were identified in miRNet, miRecords, and miRTarbase databases. Out of 12 DEMs, only six DEMs (hsa-mir-501-5p, hsa-mir-92a-1-5p, hsa-mir-618, hsa-miR-935, hsa-miR-324-5p, and hsa-miR-542-3p) were present in the validated target databases. Since these databases suffer from high false-positive rate, the six DEMs and their

26 validated target genes were reconfirmed with the literature (Table S2). Therefore 388 (362 predicted genes and 26 validated genes) target genes of DEMs were used for further analysis.

3.3 | The term and pathway enrichment analysis of gene targets

The GO (Gene Ontology) term, KEGG (Kyoto Encyclopedia of Genes and Genomes), and PANTHER pathway enrichment analysis were performed by using DAVID, version 6.8 and PANTHER database. The list of 123 predicted gene targets and 12 validated gene targets for the two upregulated DEMs and 239 predicted gene targets and 14 validated gene targets for the 10 downregulated DEMs were submitted for enrichment analysis in DAVID database.

During the GO term and pathway enrichment analysis, the 135 gene targets for upregulated DEMs and 253 gene targets for the downregulated DEMs were functionally annotated for the enrichment analysis by the databases. From the annotated gene targets, 72 gene targets of upregulated DEMs and 74 gene targets of downregulated DEMs were enriched for more than five-fold enrichment

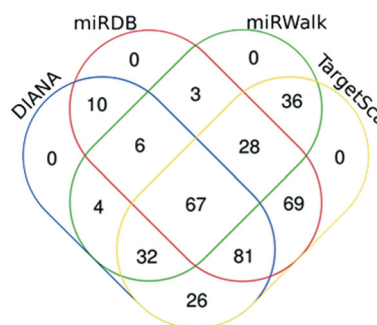


FIGURE 2 The Venn diagram representing the intersection of putative gene targets in TargetScan, miRWalk, DIANA micro-T, and miRDB. The numbers in the figure represent the number of genes common in the target prediction databases

value ($P < 0.05$) (Tables S3 and S4). The enrichment analysis classified the target genes based on their biological processes, molecular functions, cellular component, and pathways (Figures S2 and S3).

The protein abundance of randomly selected enriched genes (miR-542-3p-AKT, miR-3687-TRAF3, TRIM21, and miR-1273f-PTEN) from the pool of 146 enriched target genes showed the genes obtain after enrichment analysis is 99% confident (Figure 3C). The 12 DEMs and 146 enriched target genes were selected for further analysis (Figure 3).

3.4 | The construction of the miRNA-mRNA interaction network and identification of hub miRNAs

The enriched 12 DEMs and their corresponding 146 gene targets have been summarized in miRNA-mRNA interaction network (Figure 4 and Table S5). The visualization of the interaction network was accomplished by using Cytoscape version 3.6.1. The network for upregulated

DEMs contained 72 direct interactions with 74 nodes (two upregulated DEMs and 72 genes) and the network for downregulated DEMs contained 76 direct interactions for 84 nodes (10 downregulated and 74 genes) (Figure 4 and Table S5). According to graph theoretic network analysis, the upregulated DEMs, hsa-miR-542-3p, hsa-miR-3607, and the downregulated DEMs hsa-miR-92a-1-5p, hsa-miR-1273f, hsa-miR-3187, and hsa-miR-2682-3p were the hub miRNAs on the basis of degree centrality (higher than 7).

Therefore, the hub miRNAs can be the key molecules involved in the molecular pathogenesis of CHPV infection in human microglial cells.

3.5 | Weighted gene coexpression network analysis

The weighted gene coexpressed network of the 146 target genes obtained through enrichment analysis was constructed using the

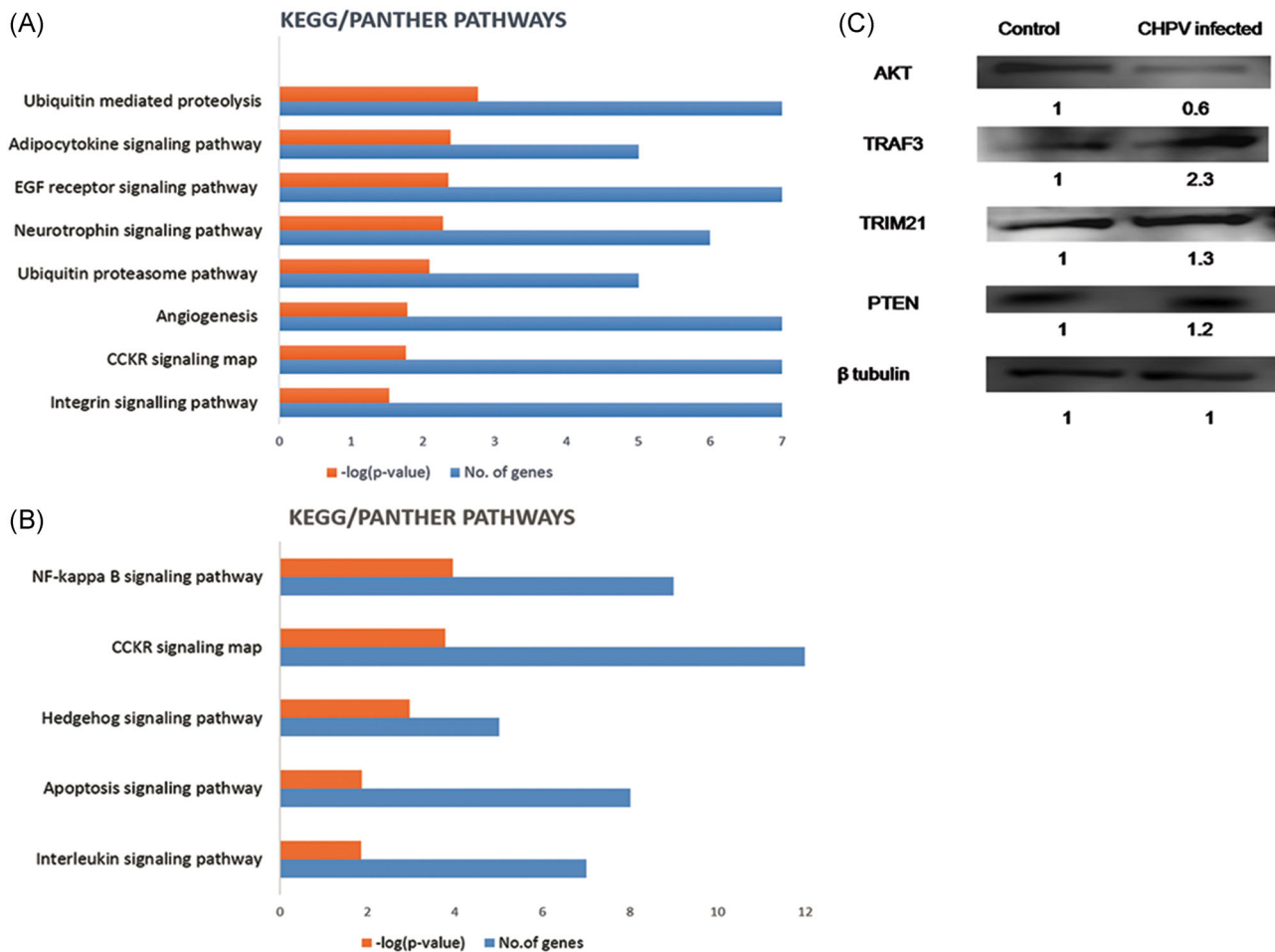


FIGURE 3 Enrichment analysis. A, The X-axis represents enriched pathways in KEGG/PANTHER databases of gene targets of upregulated miRNA of CHPV-infected human microglial cells. The Y-axis denotes the target gene counts and $-\log(P)$ value of the enriched pathways. B, The X-axis represents enriched pathways in KEGG/PANTHER databases of gene targets of downregulated miRNA of CHPV-infected human microglia. The Y-axis denotes the target gene counts and $-\log(P)$ value of the enriched pathways. C, Western blot analysis for randomly selected enriched genes (AKT, TRAF3, TRIM21, and PTEN) were at 99% confidence and 10% confidence interval obtained from the enrichment analysis data. β -Tubulin was used for normalization. The average fold change with respect to control has been mentioned. CHPV, Chandipura virus; KEGG, Kyoto Encyclopedia of Genes and Genomes; miRNA, microRNA

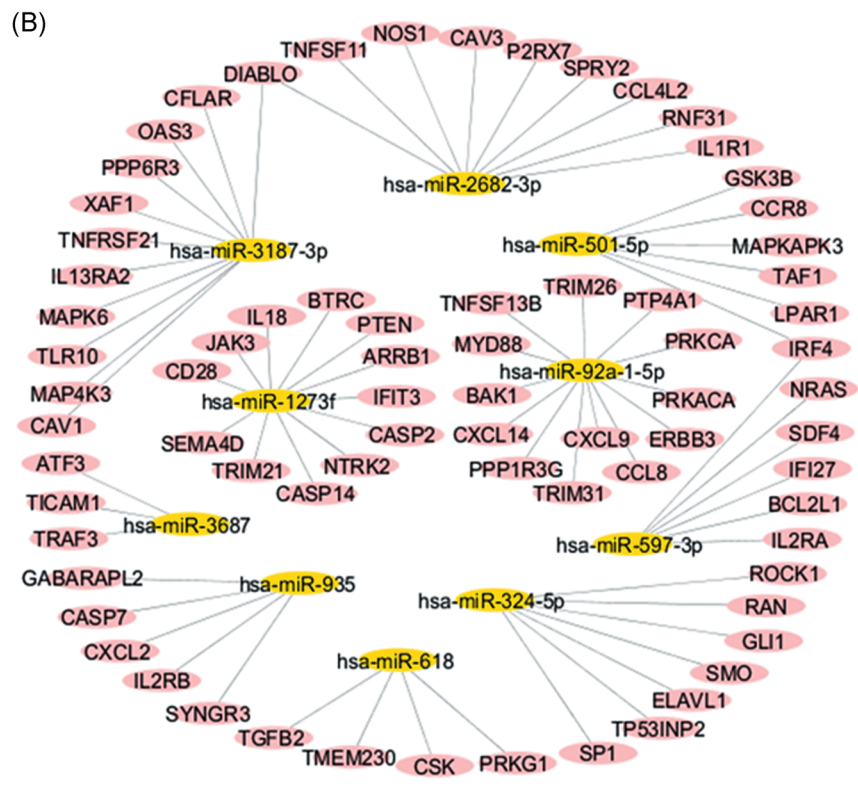
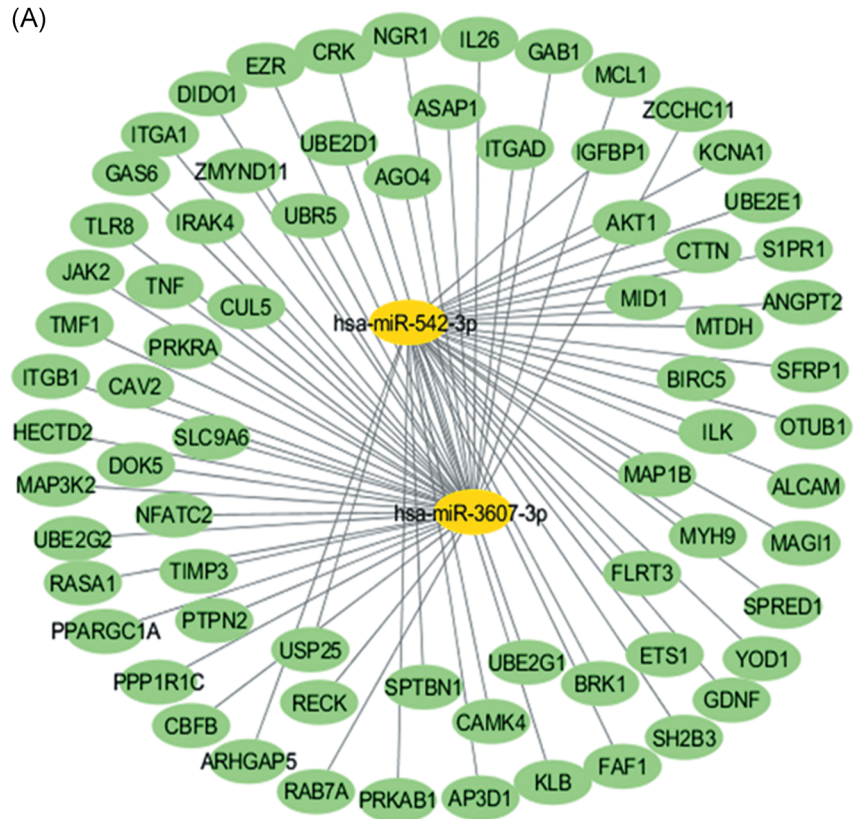


FIGURE 4 The miRNA-mRNA interaction network. A, The upregulated DEMs and their interaction with their enriched target genes in CHPV-infected human microglial cells. The yellow circles represent differentially expressed miRNAs and green circles represent their target genes. B, The downregulated miRNAs, and interaction with their target genes in CHPV-infected human microglial cells. The yellow circles represent differentially expressed miRNAs and pink circles represent their target genes. Lines represent inverse regulatory relation between DEMs and target genes. CHPV, Chandipura virus; DEM, differentially expressed miRNA; miRNA, microRNA; mRNA, messenger RNA

WGCNA package in R environment.¹³ The gene expression profile of 146 target genes of CHPV-infected human microglial cells, were highly correlated ($r > 0.3$, $P < 0.05$) with the gene expression profile of LASV (GSE41752), VSV (GSE44331), and IFN- γ (GSE1432) induced

in vivo models (Figure 5A). Weighted gene coexpressed network was constructed in the scale-free topology for the enriched 146 gene targets using the soft-power threshold value of 4. The weighted gene coexpression and the interconnected network was exported to

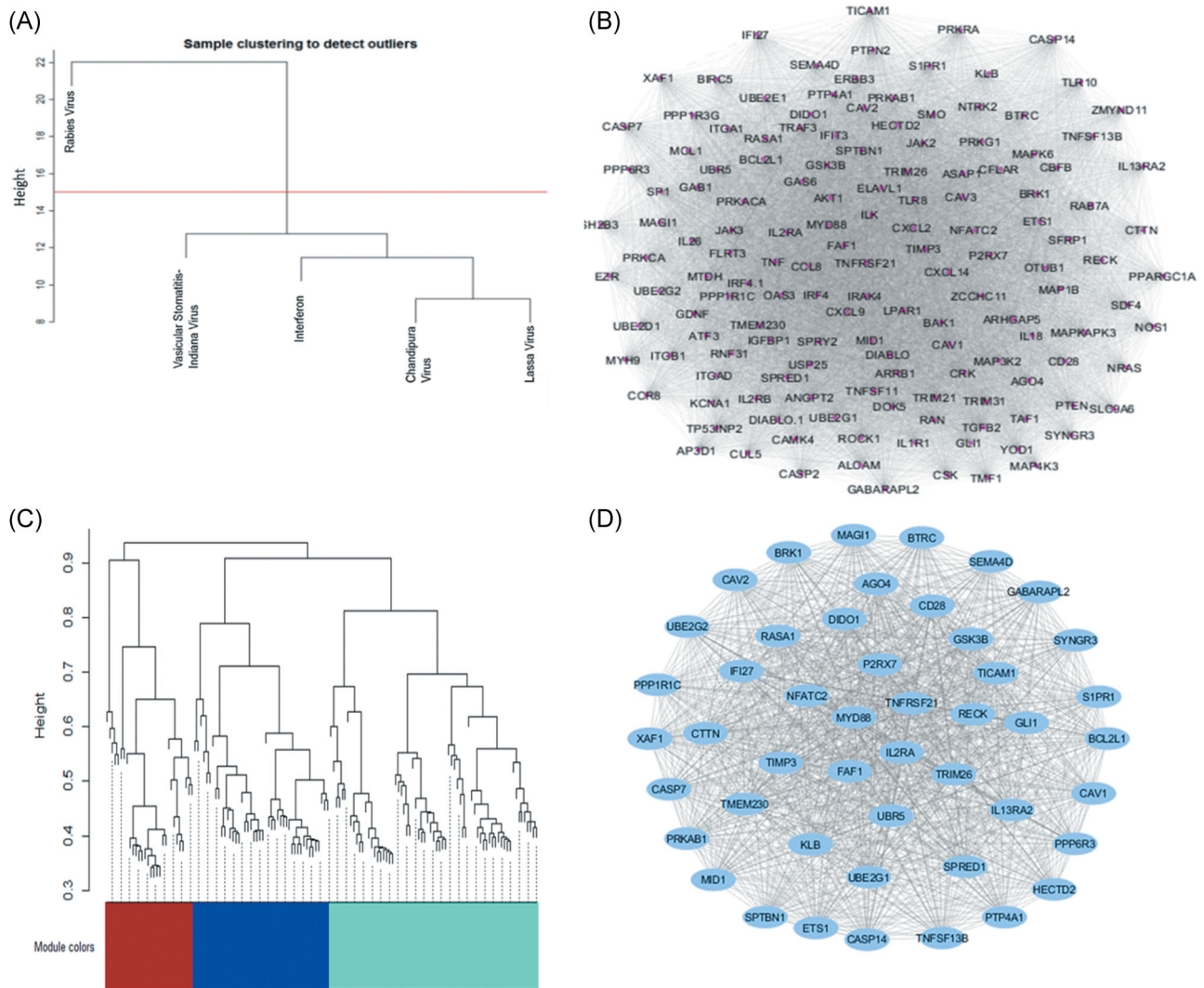


FIGURE 5 WGCNA and module analysis. A, The dendrogram represents the sample clustering during LASV, RABV, VSV, CHPV, and IFN- γ induced in vivo models. The gene expression profile of CHPV-infected human microglial cells correlated with LASV, VSV, and IFN- γ induced in vivo models. B, A weighted gene coexpressed network of enriched target genes associated with CHPV-infected human microglial cells. The network comprises 146 potential target genes and 9818 connections obtained from Cytoscape version 3.6.1. The network signifies an interconnected gene expression during CHPV-infected human microglial cells. C, Hierarchical clustering of the enriched target genes associated with CHPV-infected human microglial cells. The dendrogram plot identifies three topological scale-free modules (brown, blue, and turquoise). D, The network represents the 47 coexpressed genes in blue module with 1081 connections. CHPV, Chandipura virus; IFN- γ , interferon- γ ; LASV, Lassa virus; RABV, Rabies virus; VSV, vesicular stomatitis virus; WGCNA, weighted gene coexpression network analysis

Cytoscape version 3.6 to visualize the 146 genes and 9818 connections (Figure 5B).

3.6 | Module identification and analysis

The WGCNA network resulted in three robust and discrete modules, represented by brown, blue, and turquoise colors and these modules were formed due to dissimilarity in the inter-connectedness of the network (Figure 5C). The modules were visualized by Cytoscape version 3.6 in which brown, blue, and turquoise module comprised of 30, 47, and 69 genes, respectively. The expression levels of each module have been summarized by their first principal component

termed as module eigengene values (kME), kME brown = 0.852, kME blue = 0.431, and kME turquoise = 0.09.

The comparison of three modules with the gene expression profiles of the TNF- α (GSE45880) and IFN- γ (GSE3920) induced astrocytes and endothelial cells suggested that the kME values of a blue module having the highest correlation. The hub genes of the blue module were identified based on the position of genes and intra-modular connectivity over 0.95 ($P < 0.05$) in the network; which revealed the functional relevance of the blue module during neuroinflammation in CHPV-infected human microglial cells (Figure 5D). The hub genes of the blue module, FAF1, TNFRSF21, MYD88, and IL2RA were enriched for the

apoptosis and inflammation (FDR, $P < 0.001$). The hub genes FAF1, TNFRSF21, MYD88, and IL2RA might be the targets of hsa-miR-542-3p, hsa-miR-3187-3p, hsa-miR-92a-1-5p, and hsa-miR-597-3p, respectively.

4 | DISCUSSION

CHPV-infected patients show symptoms similar to encephalitis which can be due to elevated proinflammatory and antiviral responses (TNF- α , IFN- γ , MCP-1, IL-10, IL-6, iNOS, and COX-2).^{7,14} The human microglial cells are the resident macrophages of the CNS and extensively involved in immune surveillance, phagocytosis, and antigen presentation.⁵ The microglial activation and the bystander killing of neurons have been highlighted in previous reports.^{1,6,14} The present study reported the infection of CHPV in human microglial cells (Figure 1A) through plaque assay and perturbation of miRNA expression profile during CHPV infection (Table 1). To gain insights into the functional aspects of miRNA perturbation, the target gene prediction analysis and gene functional enrichment analysis was performed.

Out of the 12 DEMs, eight have been (hsa-miR-3607, hsa-miR-512-3p, hsa-miR-618, hsa-miR-597-3p, hsa-miR-92a-1-3p, hsa-miR-935, hsa-miR-501-5p, and hsa-miR-324-5p) previously reported in cancers, melanoma, osteosarcoma, neuroblastoma, and muscle regeneration, integrity of BBB, and virus replication,¹⁵⁻²² while four DEMs (hsa-miR-1273f, hsa-miR-3687, hsa-miR-2682, and hsa-miR-3187) have not been documented in any of the pathological conditions yet. The present study predicts the diverse role of 12 DEMs in CHPV-infected human microglial cells. The top-ranked seven predicted gene targets from miRNA gene prediction databases (MARCKSL1, IL7R, PTPN2, MAP4K3, LPAR1, ILK, and ELAVL1) have been previously reported in virus internalization, virus replication, and immune responses.^{23,24} Further, the genes ILK and ELAVL1 are the validated targets of miRNA hsa-miR-542-3p and hsa-miR-324-5p, respectively.^{25,26} In addition, the four genes (TRAF3, PTEN, AKT, and TRIM21) from the enriched target gene sets have been randomly selected to show the stability and reliability of the predicted target genes by intersection method (Figure 3C).

The ssRNA viruses such as human immunodeficiency virus and simian immunodeficiency virus are known to exploit the cell-surface receptors (TLR2, CXCR4, and CCR5) expressed on microglial cells for their entry.²⁷⁻²⁹ The induction of the surface chemokine receptors may be a strategy for a virus to enter in host cells.^{30,31} The suppression of hsa-miR-501-5p and hsa-miR-935 during CHPV infection in microglial cells may induce the expression of CCR8 and CXCL2 genes (Figure 4B). The virus hijacks the host cellular machinery by targeting several genes after entering into the cell for their replication.^{24,32-35} The sirtuins (SIRT1 and SIRT2) bind to the promoter region of the viral genome to promote virus replication by inducing the host transcription factor AP1.³⁶ In the present study, SIRT2 is the putative gene target of downregulated hsa-miR-92a-1-5p. The TNFRSF21 is the member of TNF receptor superfamily; which facilitates virus replication through AKT signaling.³⁷ The TNFRSF21 targeted by hsa-miR-3187-3p, which may promote the virus replication. Therefore, the modulation of

miRNA-mRNA pairs (hsa-miR-501-5p-CCR8, hsa-miR-935-CXCL2, hsa-miR-92a-1-5p-SIRT2, and hsa-miR-3187-3p-TNFRSF21) may facilitate virus entry, replication and propagation to successfully establish CHPV infection in microglial cells.

The WGCNA provided inter-connectedness among the enriched genes (146 genes), which may help in understanding the CHPV-mediated pathogenesis (Figure 5B). The enriched gene sets in our data include chemokine and cytokine receptors (CCL8, CCL4L2, CCR8, CXCL2, CXCL9, and CXCL14), calcium ions signaling (P2RX7, ELAV1, and BAK1) and zinc finger proteins (PTPN2, ZCCHC11, and NFATC2), which might play roles in CHPV pathogenesis by activating microglial cells.^{38,39} In addition, the previous reports have shown the increased levels of pro-inflammatory cytokines (TNF- α , IFN- γ , IL-6, IL-10, MCP-1, IL-1 β , and IL-8) and chemokines (CXCL9, CCL5, CCL2, and CXCL10) in CHPV-infected mice, which led to neuroinflammation, neurotoxicity, and neuronal death.^{6,14,40} Therefore, It is believed that the activation of microglial cells play a pivotal role in promoting neuroinflammation during CHPV infection.¹⁴

The activated microglial cells use multiple defense mechanisms against virus infection. The microglial cells express pattern recognition receptors like toll-like receptor, dead box helicases, RIG-I, and MDA5, which sense the RNA viruses.⁴¹ The toll-like receptors mediate antiviral response through the activation of interferon-stimulated genes) like OAS, TRIM21, IFIT27, and IFIT3 (Table S4).⁴² The antiviral OAS3 gene from enrichment analysis has been previously reported to tag the viral double-stranded RNAs with 2',5' adenosine oligomers, followed by RNase L-mediated degradation of the viral RNA.⁴³ The OAS3 gene has been predicted as putative target of the downregulated, hsa-miR-3187-3p, which may promote the antiviral interferon response (IFN- α and - γ) (Figure 4B). In addition, TRIM21 has been reported to upregulate during CHPV infection in microglial cells (Figure 3C), which is a putative target of downregulated, hsa-miR-1273f (Figure 4B). It is implied from the network analysis and other studies that CHPV infection is a powerful trigger for interferon (IFN- γ) response.^{14,40}

The aggravated expression of TNF- α and IFN- γ act as a pathological trait for neuroinflammatory events during CHPV infection.⁷ In addition, the human rTNF- α and rIFN- γ have been studied in mice models for the neuroinflammation.^{44,45} The modular analysis of WGCNA demonstrated the blue module, which highly correlated to the gene expression profile of TNF- α and IFN- γ induced cells (Figure 5D). The hub genes of the blue module, FAF1, TNFRSF21, MYD88, and IL2RA were enriched for apoptosis and inflammation, which may be the inflammatory genes involved during CHPV-infection in human microglial cells.

The hub genes in the blue module are mostly involved in nuclear factor- κ B (NF- κ B) activity. Further, the activation of NF- κ B activity has been reported in CHPV-infected microglial cells.⁶ The elevated levels of TNF- α , IFN- γ , IL-2, IL-6, CCL2, IL-1 β , IL-8 CCL5, and IL-10 in mice may be due to the activation of NF- κ B signaling.^{6,7,26} In addition, pathway enrichment analysis revealed the over-representation of the NF- κ B pathway during CHPV infection (Figure 3B). The increase in the expression levels of NF- κ B transcription factor in microglial cells

during CHPV infection may affect the transcription of several chemokines, cytokines, and pro-inflammatory factors.

The involvement of the gene FAF1 has been reported in the proteasomal degradation, chaperone activity, and NF- κ B activity.⁴⁶ The data from module analysis suggested that the suppression of FAF1 by hsa-miR-542-3p might lead to the activation of NF- κ B signaling. The increased expression levels of TNFRSF21, IL2RA, and MYD88 leads to activation of NF- κ B signaling through TRADD/ TRAF2 pathway, JAK/PI3K/AKT pathway, and the mitogen-activated protein kinase pathway, respectively.⁴⁷⁻⁵⁰ The ectopic expression of TNFRSF21, MYD88, and IL2RA may be modulated by downregulated hsa-miR-3187-3p, hsa-miR-92a-1-5p, and hsa-miR-597-3p, respectively. These miRNA-mRNA interactions may activate NF- κ B signaling; which may further lead to a feed-forward loop of neuroinflammatory responses during CHPV infection in activated microglia. The overexpression of hub miRNAs hsa-miR-92a-1-5p and hsa-3187-3p, and knockdown of hsa-miR-542-3p can be a protective strategy adopted by CHPV to suppress neuroinflammatory events during the course of infection in human microglial cells by targeting respective target hub genes MYD88, TNFRSF21, and FAF1.

The in silico analysis of the microRNA data generated for the CHPV-infected human microglial cells provided the molecular basis of the neuroinflammatory events during the infection. The genome-wide analysis supported previous findings of microglial activation and immune dysregulation through statistical assessment analysis of transcriptional alterations due to miRNA expression level. Altogether, the present study will be helpful in understanding the molecular networks/pathways exploited by CHPV in microglial cells through the microRNAs.

ACKNOWLEDGMENTS

The authors highly acknowledge the funding received by the Department of Biotechnology, Ministry of Science and Technology, Govt. of India, (BT/PR27501/MED/122/142/2018). AB is the recipient of Tata Innovation Fellowship (BT/HRD/35/01/02/2014) from the Department of Biotechnology, Ministry of Science and Technology, Govt. of India.

CONFLICT OF INTERESTS

The authors declare that there is no conflict of interests.

AUTHOR CONTRIBUTIONS

MA and MR performed the bioinformatics analysis, conducted the supporting experiments, and wrote the manuscript; SD and NP helped in designing the experiment and provided technical support in data analysis. AB provided the various reagents and samples, SKS conceived the idea, supervised the experimental design, and data analysis.

ETHICS STATEMENT

The study has been conducted by following established protocols with the compliance to ethical standards.

ORCID

Sunit K. Singh  <http://orcid.org/0000-0002-8802-1169>

REFERENCES

- Ghosh S, Dutta K, Basu A. Chandipura virus induces neuronal death through Fas-mediated extrinsic apoptotic pathway. *J Virol.* 2013;87(22):12398-12406.
- Rao BL, Basu A, Wairagkar NS, et al. A large outbreak of acute encephalitis with a high fatality rate in children in Andhra Pradesh, India, in 2003, associated with Chandipura virus. *Lancet (London, England).* 2004;364(9437):869-874.
- Cherian SS, Gunjekar RS, Banerjee A, Kumar S, Arankalle VA. Whole genomes of Chandipura virus isolates and comparative analysis with other rhabdoviruses. *PLoS One.* 2012;7(1):e30315.
- McGavern DB, Kang SS. Illuminating viral infections in the nervous system. *Nat Rev Immunol.* 2011;11(5):318-329.
- Rastogi M, Srivastava N, Singh SK. Exploitation of microRNAs by Japanese Encephalitis virus in human microglial cells. *J Med Virol.* 2018;90(4):648-654.
- Verma AK, Waghmare TS, Jachak GR, Philkhana SC, Reddy DS, Basu A. Nitrosporeusine analogue ameliorates Chandipura virus induced inflammatory response in CNS via NFKappab inactivation in microglia. *PLoS Neglected Trop Dis.* 2018;12(7):e0006648.
- Balakrishnan A, Mishra AC. Immune response during acute Chandipura viral infection in experimentally infected susceptible mice. *Virol J.* 2008;5:121.
- Singh SK, Pal Bhadra M, Girschick HJ, Bhadra U. MicroRNAs--micro in size but macro in function. *FEBS J.* 2008;275(20):4929-4944.
- Sharma N, Verma R, Kumawat KL, Basu A, Singh SK. miR-146a suppresses cellular immune response during Japanese encephalitis virus JaOAR5982 strain infection in human microglial cells. *J Neuroinflammation.* 2015;12(1):30.
- Sharma N, Kumawat KL, Rastogi M, Basu A, Singh SK. Japanese Encephalitis virus exploits the microRNA-432 to regulate the expression of suppressor of cytokine signaling (SOCS) 5. *Sci Rep.* 2016;6:27685-27685.
- Mishra R, Chhatbar C, Singh SK. HIV-1 Tat C-mediated regulation of tumor necrosis factor receptor-associated factor-3 by microRNA 32 in human microglia. *J Neuroinflammation.* 2012;9:131-131.
- Arora A, Simpson DA. Individual mRNA expression profiles reveal the effects of specific microRNAs. *Genome Biol.* 2008;9(5):R82.
- Zhang B, Horvath S. A general framework for weighted gene co-expression network analysis. *Stat Appl Genet Mol Biol.* 2005;4:1-43.
- Verma AK, Ghosh S, Pradhan S, Basu A. Microglial activation induces neuronal death in Chandipura virus infection. *Sci Rep.* 2016;6:22544.
- Lin Y, Gu Q, Sun Z, et al. Upregulation of miR-3607 promotes lung adenocarcinoma proliferation by suppressing APC expression. *Biomed Pharmacother.* 2017;95:497-503.
- Chen F, Zhu HH, Zhou LF, Wu SS, Wang J, Chen Z. Inhibition of c-FLIP expression by miR-512-3p contributes to taxol-induced apoptosis in hepatocellular carcinoma cells. *Oncol Rep.* 2010;23(5):1457-1462.
- Chen Y, Du M, Chen W, et al. Polymorphism rs2682818 in miR-618 is associated with colorectal cancer susceptibility in a Han Chinese population. *Cancer Med.* 2018;7(4):1194-1200.

18. Lin Z, Tang Y, Tan H, Cai D. MicroRNA-92a-1-5p influences osteogenic differentiation of MC3T3-E1 cells by regulating beta-catenin. *J Bone Miner Metab.* 2018;37:264-272.
19. He J, Mai J, Li Y, et al. miR-597 inhibits breast cancer cell proliferation, migration and invasion through FOSL2. *Oncol Rep.* 2017;37(5):2672-2678.
20. Yang M, Cui G, Ding M, et al. miR-935 promotes gastric cancer cell proliferation by targeting SOX7. *Biomed Pharmacother.* 2016;79:153-158.
21. de Stephanis L, Mangolini A, Servello M, et al. MicroRNA501-5p induces p53 proteasome degradation through the activation of the mTOR/MDM2 pathway in ADPKD cells. *J Cell Physiol.* 2018;233(9):6911-6924.
22. Lin H, Zhou AJ, Zhang JY, Liu SF, Gu JX. MiR-324-5p reduces viability and induces apoptosis in gastric cancer cells through modulating TSPAN8. *J Pharm Pharmacol.* 2018;70(11):1513-1520.
23. Kong F, Hu W, Zhou K, et al. Hepatitis B virus X protein promotes interleukin-7 receptor expression via NF-kappaB and Notch1 pathway to facilitate proliferation and migration of hepatitis B virus-related hepatoma cells. *J Exp Clin Cancer Res.* 2016;35(1):172.
24. Farquhar MJ, Humphreys IS, Rudge SA, et al. Autotaxin-lysophosphatidic acid receptor signalling regulates hepatitis C virus replication. *J Hepatol.* 2017;66(5):919-929.
25. Shwetha S, Kumar A, Mullick R, Vasudevan D, Mukherjee N, Das S. HuR displaces polypyrimidine tract binding protein to facilitate LA binding to the 3' untranslated region and enhances hepatitis C virus replication. *J Virol.* 2015;89(22):11356-11371.
26. Qiao B, Cai JH, King-Yin Lam A, He BX. MicroRNA-542-3p inhibits oral squamous cell carcinoma progression by inhibiting ILK/TGF-beta1/Smad2/3 signaling. *Oncotarget.* 2017;8(41):70761-70776.
27. Bolduc JF, Ouellet M, Hany L, Tremblay MJ. Toll-like receptor 2 ligation enhances HIV-1 replication in activated CCR6+ CD4+ T cells by increasing virus entry and establishing a more permissive environment to infection. *J Virol.* 2017;91(4):e01402-e01416.
28. Schramm B, Penn ML, Speck RF, et al. Viral entry through CXCR4 is a pathogenic factor and therapeutic target in human immunodeficiency virus type 1 disease. *J Virol.* 2000;74(1):184-192.
29. Hill CM, Deng H, Unutmaz D, et al. Envelope glycoproteins from human immunodeficiency virus types 1 and 2 and simian immunodeficiency virus can use human CCR5 as a coreceptor for viral entry and make direct CD4-dependent interactions with this chemokine receptor. *J Virol.* 1997;71(9):6296-6304.
30. Lee S, Tiffany HL, King L, Murphy PM, Golding H, Zaitseva MB. CCR8 on human thymocytes functions as a human immunodeficiency virus type 1 coreceptor. *J Virol.* 2000;74(15):6946-6952.
31. Wareing MD, Lyon AB, Lu B, Gerard C, Sarawar SR. Chemokine expression during the development and resolution of a pulmonary leukocyte response to influenza A virus infection in mice. *J Leukoc Biol.* 2004;76(4):886-895.
32. Huber M, Suprunenko T, Ashhurst T, et al. IRF9 prevents CD8(+) T cell exhaustion in an extrinsic manner during acute lymphocytic choriomeningitis virus infection. *J Virol.* 2017;91(22):e01219-17.
33. Jheng JR, Lau KS, Lan YW, Horng JT. A novel role of ER stress signal transducer ATF6 in regulating enterovirus A71 viral protein stability. *J Biomed Sci.* 2018;25(1):9.
34. Franz KM, Neidermyer WJ, Tan YJ, Whelan SPJ, Kagan JC. STING-dependent translation inhibition restricts RNA virus replication. *Proc Natl Acad Sci USA.* 2018;115(9):E2058-E2067.
35. Esfandiari M, Suarez A, Amaral A, et al. Novel role for integrin-linked kinase in modulation of coxsackievirus B3 replication and virus-induced cardiomyocyte injury. *Circ Res.* 2006;99(4):354-361.
36. Yang CH, Li HC, Ku TS, et al. Hepatitis C virus down-regulates SERPINE1/PAI-1 expression to facilitate its replication. *J Gen Virol.* 2017;98(9):2274-2286.
37. Luong TTD, Tran GVQ, Shin DJ, Lim YS, Hwang SB. Hepatitis C virus exploits death receptor 6-mediated signaling pathway to facilitate viral propagation. *Sci Rep.* 2017;7(1):6445.
38. Song GJ, Kim J, Kim JH, et al. Comparative analysis of protein tyrosine phosphatases regulating microglial activation. *Exp Neurobiol.* 2016;25(5):252-261.
39. Mizoguchi Y, Monji A. Microglial intracellular Ca(2+) signaling in synaptic development and its alterations in neurodevelopmental disorders. *Front Cell Neurosci.* 2017;11:69.
40. Anukumar B, Shahir P. Chandipura virus infection in mice: the role of toll like receptor 4 in pathogenesis. *BMC Infect Dis.* 2012;12:125.
41. Okamoto M, Tsukamoto H, Kouwaki T, Seya T, Oshiumi H. Recognition of viral RNA by pattern recognition receptors in the induction of innate immunity and excessive inflammation during respiratory viral infections. *Viral Immunol.* 2017;30(6):408-420.
42. Schneider P, Weber-Fahr W, Schweinfurth N, et al. Central metabolite changes and activation of microglia after peripheral interleukin-2 challenge. *Brain Behav Immun.* 2012;26(2):277-283.
43. Li Y, Banerjee S, Wang Y, et al. Activation of RNase L is dependent on OAS3 expression during infection with diverse human viruses. *Proc Natl Acad Sci USA.* 2016;113(8):2241-2246.
44. Karamita M, Barnum C, Tesi R, Szymkowski D, Tansey M, Probert L. Inhibition of soluble TNF protects mice against brain inflammation and demyelination in a cuprizone model for multiple sclerosis. *J Neuroimmunol.* 2014;275(1):182.
45. Gresa-Arribas N, Vieitez C, Dentesano G, Serratosa J, Saura J, Sola C. Modelling neuroinflammation in vitro: a tool to test the potential neuroprotective effect of anti-inflammatory agents. *PLOS One.* 2012;7(9):e45227.
46. Park MY, Jang HD, Lee SY, Lee KJ, Kim E. Fas-associated factor-1 inhibits nuclear factor-kappaB (NF-kappaB) activity by interfering with nuclear translocation of the RelA (p65) subunit of NF-kappaB. *J Biol Chem.* 2004;279(4):2544-2549.
47. Zhang D, Cao X, Li J, Zhao G. MiR-210 inhibits NF-kappaB signaling pathway by targeting DR6 in osteoarthritis. *Sci Rep.* 2015;5:12775.
48. McDonald JU, Zhong Z, Groves HT, Tregoning JS. Inflammatory responses to influenza vaccination at the extremes of age. *Immunology.* 2017;151(4):451-463.
49. Shatrova AN, Mityushova EV, Vassilieva IO, et al. Time-dependent regulation of IL-2R alpha-chain (CD25) expression by TCR signal strength and IL-2-induced STAT5 signaling in activated human blood T lymphocytes. *PLOS One.* 2016;11(12):e0167215.
50. Rajalakshmy AR, Malathi J, Madhavan HN. Hepatitis C virus NS3 mediated microglial inflammation via TLR2/TLR6 MyD88/NF-kappaB pathway and toll like receptor ligand treatment furnished immune tolerance. *PLOS One.* 2015;10(5):e0125419.

SUPPORTING INFORMATION

Additional supporting information may be found online in the Supporting Information section at the end of the article.

How to cite this article: Agrawal M, Rastogi M, Dogra S, Pandey N, Basu A, Singh SK. Chandipura virus changes cellular miRNome in human microglial cells. *J Med Virol.* 2019;1-11. <https://doi.org/10.1002/jmv.25491>